

Synthesis and Characterization of Fe and Ni Co-Doped $\text{Ba}_{0.6}\text{Sr}_{0.4}\text{TiO}_3$ Prepared by Sol-Gel Technique

Naghi Shaban^{1*} and Mahmood Bahar^{1,2}

¹Department of Physics, Kharazmi University, Tehran, Iran

²Department of Physics, Islamic Azad University, Tehran North Branch, Tehran, Iran

Abstract

In this research work, Influence of Fe and Ni dopant on structural $\text{Ba}_{0.6}\text{Sr}_{0.4}\text{TiO}_3$ nanocrystalline was studied. The pure and (Fe and Ni)-doped $\text{Ba}_{0.6}\text{Sr}_{0.4}\text{TiO}_3$ ($\text{Ba}_{1-x}\text{Sr}_x\text{TiO}_3$, where $(x=0.4)$, $\text{Ba}_{1-x}\text{Sr}_x\text{Ti}_{1-y}\text{Fe}_y\text{O}_3$, where $(x=0.4, y=0.1)$ and $\text{Ba}_{1-x}\text{Sr}_x\text{Ti}_{1-y}\text{Ni}_y\text{O}_3$, where $(x=0.4, y=0.1)$) in powder, abbreviated as (BST), (BSTF) and (BSTN), respectively were prepared by a modified Sol-gel technique. In this process, stoichiometric proportions of barium acetate and strontium acetate were dissolved in acetic acid and titanium (IV) isopropoxide was added to form BST gel. The as-formed gels were dried at 200°C and then calcined at 850°C for crystallization. In order to improved crystallization, surface morphology and optimized grain size used Fe^{+3} and Ni^{2+} ions. Samples were characterized by Infrared spectroscopy method (FT-IR), UV-Visible spectroscopy, X-Ray Diffraction technique (XRD), Field Emission Scanning Electron Microscope (FESEM) and Energy Dispersive X-Ray Spectroscopy (EDS). The Nano-scale presence and the formation of the cubic perovskite phase as well as the crystallinity were detected using the mentioned techniques. The results showed that, the adding Fe and Ni to BST structure lead to decrease of the average size of nanoparticles and change the optical properties of the BST. The nanocrystallite sizes obtained were nearly 38, 37 and 34 nm, for BST, BSTF and BSTN powders calcined at 850°C, respectively.

Keywords: Sol-gel; $\text{Ba}_{0.6}\text{Sr}_{0.4}\text{TiO}_3$; Nanocrystalline; Iron doping; Nickel doping

Introduction

Barium-Strontium Titanate (BST) is an important ceramic oxide with the perovskite structure and stoichiometric formula $\text{Ba}_x\text{Sr}_{1-x}\text{TiO}_3$. Recently, barium strontium titanate (BST) have been widely investigated because of its high dielectric constant, nonlinear variation of dielectric constant with the electric field, ferroelectricity, pyroelectric properties and so on. The desired properties make BST a promising candidate material for tunable microwave dielectric devices such as multilayer and voltage-tunable capacitors, dynamic random access memories (DRAM), microwave phase shifters, tunable filters, oscillators, uncooled infrared sensors and etc. [1-3]. Among of all compositions of BST, the $\text{Ba}_{0.6}\text{Sr}_{0.4}\text{TiO}_3$ compound because of its good combination of low T_c , high dielectric constant, relatively low loss tangent and better tunability is a particular importance stoichiometry [4,5].

It is well-known that Ferroelectric and dielectric properties of BST ceramics are strongly dependent on the sintering conditions, grain size, porosity, doping amount of various concentrations and structural defects. Some materials that can improve the listed properties have been tried in the doping. Among these, materials can be noted to Some dopants including, Co^{2+} , Mn^{2+} , Mn^{3+} , Fe^{2+} , Fe^{3+} , Co^{2+} , Co^{3+} , Ni^{2+} , Cr^{3+} , Mg^{2+} , Al^{3+} , Ga^{3+} , etc., which can occupy the B sites of the ABO_3 perovskite structure [6-8].

Various preparation methods for BST have been investigated such as solid-state reaction [9], sol-gel [7,10,11], hydrothermal [12,13], spray pyrolysis [14], combustion synthesis [15], and chemical co-precipitation methods [16] and etc. Compared with other methods, sol-gel process because of its numerous advantages in producing barium-strontium titanate ceramics has received a strong attention among researchers. Among these advantages, low temperature of this process, possibility for obtaining nanostructures, easy control of microstructure and the crystallization rate of the final product, lower pollution and low cost of operation can be noted [17,18].

In this research, we aim to synthesize nanocrystalline pure BST and (Fe and Ni) co-doping into the BST structure via a modified sol-gel process and investigate the structural of BST samples in powder form, by doping with 10 mole% Fe^{+3} and Ni^{2+} ions doped BST ceramics. The Fe^{+3} and Ni^{2+} ions substitute at Ti^{4+} site in BST structure and study of influence of them to microstructure. The structure and the morphology of the prepared samples will be evaluated by using FT-IR, XRD and FESEM.

Materials and Methods

Nano-structure pure barium strontium titanate, $\text{Ba}_{1-x}\text{Sr}_x\text{TiO}_3$, where $(x=0.4)$ (BST) and doped with Fe^{+3} and Ni^{2+} ions, $\text{Ba}_{1-x}\text{Sr}_x\text{Ti}_{1-y}\text{Fe}_y\text{O}_3$, where $(x=0.4, y=0.1)$ (BSTF) and $\text{Ba}_{1-x}\text{Sr}_x\text{Ti}_{1-y}\text{Ni}_y\text{O}_3$, where $(x=0.4$ and $y=0.1)$ (BSTN), in powder forms were prepared, by a modified sol-gel method. The samples were synthesized using barium acetate (ACS reagent grade, 99%, Merck, Germany), strontium acetate (ACS reagent grade, 99.9%, Sigma Aldrich, USA) and titanium (IV) isopropoxide (ACS reagent grade, 99.9%, Sigma Aldrich, USA) as precursors for barium, strontium and titanium, respectively. Acetic acid (Glacial, 99-100% EMPLURA, Merck, Germany) was used as solvent and ethanol (99+%, Merck, Germany) was used to stabilize Titanium (IV) isopropoxide. Iron and Nickel nitrates (ACS reagent grade, 99%, Merck, Germany) using as a precursor for Iron and nickel.

Firstly, Barium acetate and strontium acetate were mixed in a mole ratio of Ba:Sr=6:4, and then dissolved in heated glacial acetic acid with

*Corresponding author: Naghi Shaban, Department of Physics, Kharazmi University, Tehran, Iran, Tel: +982188329220; E-mail: n.shaban2014@gmail.com

Received May 24, 2017; Accepted July 29, 2017; Published August 03, 2017

Citation: Shaban N, Bahar M (2017) Synthesis and Characterization of Fe and Ni Co-Doped $\text{Ba}_{0.6}\text{Sr}_{0.4}\text{TiO}_3$ Prepared by Sol-Gel Technique. J Theor Comput Sci 4: 157. doi:10.4172/2376-130X.1000157

Copyright: © 2017 Shaban N, et al. This is an open-access article distributed under the terms of the Creative Commons Attribution License, which permits unrestricted use, distribution, and reproduction in any medium, provided the original author and source are credited.

constant stirring. Ethanol was added in Titanium (IV) isopropoxide to form a separate solution at room temperature. After cooling to room temperature, the Ba-Sr solution was added to the as prepared Ti solution drop by drop. Refluxing resulted in the formation of a thick white colored gel. The prepared gel was cooled to 5°C and deionized water was added to it and the solution was stirred magnetically for 60 min. Iron and Nickel nitrate were added to the final solution with molar ratio 10 mole %. Densification of the gels were achieved by sintering in the air for 4 hours at 850°C for BST, BSTF and BSTN samples in a muffle furnace.

The phases of the obtained samples were characterized by X-ray diffraction (XRD) (Philips X-ray diffractometer, 40 kV, 40 mA) in a wide range of Bragg's angle of 10°-85° using Cu Kα (1.5406 Å) radiation with a step size of 0.02 at room temperature. Microstructure was studied with a field emission scanning electron microscope (Mira 3-XMU). The chemical compounds of samples are characterized by Energy Dispersive X-Ray Spectroscopy (EDS) (EDS microanalyzer in FESEM, Mira 3-XMU). The FT-IR spectra of the calcined powders were recorded with an FT-IR spectrometer (Bruker Vector 33) in the range of 400-4000 cm⁻¹. Also, The UV-Visible absorption spectra of the powder samples were recorded using a UV-VIS spectrophotometer (photonix Ar 2015, Iran) in the spectral region from 200 to 800 nm at room temperature.

Results and Discussion

FT-IR analysis

Figure 1 shows the IR spectrum of BST, BSTF and BSTN powders calcined at 850°C for 4 hours. FTIR spectra for BST doped with Fe and Ni elements have the same trend for the pure BST sample. The broad band at 3422 cm⁻¹ is related to O-H stretching modes of absorbed water by KBr pellets that were used for FT-IR spectroscopy [19]. The peaks corresponding to barium carbonate were evident at 1630, 1427, 850 and 580 cm⁻¹ [20]. The absorption band at 1427 cm⁻¹ can be interpreted as C=O vibration due to extremely small unavoidable traces of carbonate. It can be seen that as the adding of Fe and Ni to BST structure, the amount of carbonates formed increases. Hence, the result shows that BST nanopowder obtained at 850°C are more pure than BSTF and BSTN at the same temperature. Furthermore, the absorption band at 611 cm⁻¹ is assigned to specific vibrations of Ti-O bonds for pure BST [21]. Also, a shoulder around 954 cm⁻¹ and a dip at 1063 cm⁻¹ appears to be getting more prominent in Fe and Ni doped BST samples corresponding to the formation of new bonds due to dopant Fe and

Ni. As can be seen, there are no new peaks appearing for the dopants (Fe³⁺ and Ni²⁺) and the only change appeared in the band for Ti-O stretching vibration at 611 cm⁻¹ for pure BST, in which it was shifted to smaller wavenumber cm⁻¹ for BSTF and BSTN, which confirm that Fe³⁺ and Ni²⁺ ions completely substitute the Ti⁴⁺ ions in the B site of the perovskite structure ABO₃ [22,23].

Phase analysis of nano powders

X-ray diffraction was performed to characterize the crystallinity and phase of the nanopowders. Figure 2 shows the XRD patterns of pure BST, BSTF and BSTN calcined in air at 850°C for 4 hours. The XRD patterns indicate that all the samples are crystalline and exhibit cubic perovskite structure with (110) as a major peak, (PDF Card No. 00-034-0411).

As was observed in previous studies, increasing the calcination temperature from 750 to 850°C leads to decompose of impurity phases of barium and strontium carbonate in pure BST [24,25]. But according to the XRD pattern shown in Figure 2, by adding impurity of iron and nickel to BST structure, an amount of impurity phase of barium carbonate remains in the composition calcined at 850°C. As can be seen, in BSTF and BSTN, XRD pattern, a weak line occurs at 24.2 which corresponds to the residual carbonates phase such as BaCO₃, SrCO₃ and (Ba,Sr)CO₃ [25]. This can be confirmed by FT-IR analysis of nano powders calcined at 850°C. However, in all samples, the predominant phase is the cubic perovskite phase of Ba_{0.6}Sr_{0.4}TiO₃. The XRD pattern of BSTF and BSTN samples conform to the cubic phase of BST and shows that there are no type of predominant impure phase and no change in the BST structure despite Fe and Ni ions in BST lattice. Due to this it can be concluded that Fe³⁺ and Ni²⁺ ions have been substituted at Ti⁴⁺ site in BST perovskite structure, appropriately as confirmed by the FT-IR obtain data.

The crystallite size (d) is determined from the Scherrer's equation:

$$\langle d \rangle = \frac{K\lambda}{\beta \cos \theta} \quad (1)$$

where K is the Scherer constant, in the present case K=0.9, λ is the wavelength and β is the full width (in radians) of the peak at half maximum (FWHM). In order to determine the lattice constant, the equation for a cubic crystal was used:

$$\sin^2 \theta = \frac{\lambda^2 (h^2 + k^2 + l^2)}{4a^2} \quad (2)$$

where α is the lattice spacing of a cubic crystal and h, k, l are the Miller indices of the Bragg plane.

Tables 1-3 shows details of the calculated X-ray spectrum for the BST, BSTF and BSTN powders calcined at 850°C. The average crystallite sizes of the samples, calculated using Scherrer's formula for the first four predominant peaks. The results show that when Fe and Ni add to BST structure, the average crystallite size has decreased. As was observed in previous studies [24], increasing the calcination temperature from 750 to 850°C leads to an increase in particle size of BST sample but, by doping Fe and Ni ions to BST despite increasing of the temperature, the crystallite size decrease, which this effect is more obvious for nickel ions.

The lattice constant was calculated for the final three peaks for larger angles. This leads to a smaller error in the calculated value of the lattice parameter. The calculated lattice parameter (a) is in good agreement with the result of the X-ray pattern fitting for BST60/40 ceramics (PDF Card No. 00-034-0411) as shown in Table 4. Also, an obvious shift in

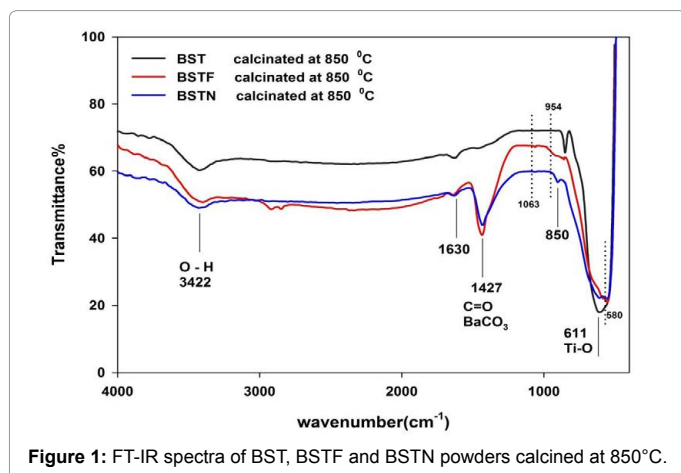


Figure 1: FT-IR spectra of BST, BSTF and BSTN powders calcined at 850°C.

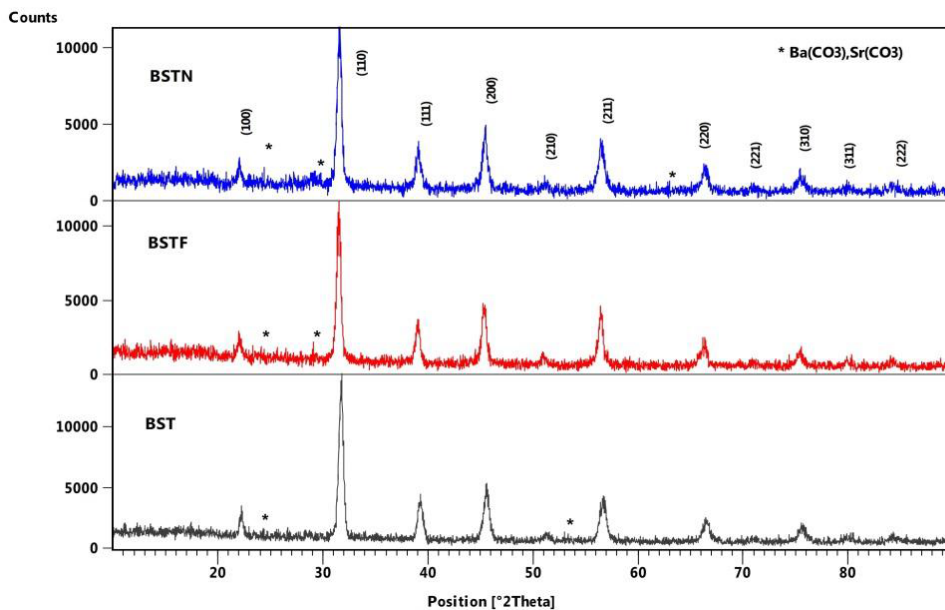


Figure 2: XRD patterns of the BST, BSTF and BSTN powders synthesize at 850°C.

h k l	2θ [deg]	d _{hkl} [Å]	FWHM [deg]	Crystal size [nm]	Lattice parameter [Å]
1 0 0	22.279	3.9869	0.1665	48.61	
1 1 0	31.826	2.8093	0.2193	37.65	
1 1 1	39.312	2.2899	0.253	33.33	
2 0 0	45.632	1.9864	0.2748	31.35	
			Average	37.74	
3 1 0	75.609	1.2566			3.972
3 1 1	80.281	1.1948			3.961
2 2 2	84.378	1.1469			3.972
				Average	3.969

Table 1: Details of the calculated X-ray spectrum for BST powder calcined at 850°C.

h k l	2θ [deg]	d _{hkl} [Å]	FWHM [deg]	Crystal size [nm]	Lattice parameter [Å]
1 0 0	22.086	4.0199	0.1969	41.09	
1 1 0	31.555	2.8319	0.2135	38.65	
1 1 1	39.143	2.2986	0.2288	36.84	
2 0 0	45.460	1.9928	0.2836	30.36	
			Average	36.73	
3 1 0	75.387	1.2568			3.9823
3 1 1	79.892	1.1993			3.9775
2 2 2	84.117	1.1494			3.9818
				Average	3.9805

Table 2: Details of the calculated X-ray spectrum for BSTF powder calcined at 850°C.

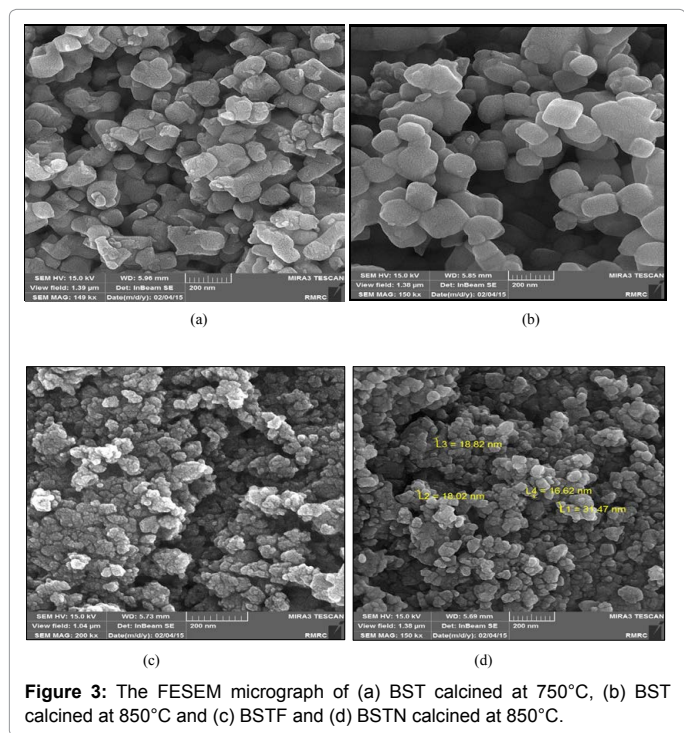
h k l	2θ [deg]	d _{hkl} [Å]	FWHM [deg]	Crystal size [nm]	Lattice parameter [Å]
1 0 0	22.122	4.0135	0.2185	37.03	
1 1 0	31.685	2.8205	0.2253	36.64	
1 1 1	39.214	2.2946	0.3348	25.18	
2 0 0	45.562	1.9886	0.2331	36.95	
			Average	33.95	
3 1 0	75.483	1.2583			3.9781
3 1 1	79.903	1.1991			3.9770
2 2 2	84.264	1.1423			3.9761
				Average	3.9770

Table 3: Details of the calculated X-ray spectrum for BSTN powder calcined at 850°C.

peaks and an increasing of lattice parameter is observed with doping of Fe and Ni ions in BST that is due to the larger radius of Fe⁺³ (0.078 nm) and Ni⁺² (0.069 nm) ions than Ti⁺⁴ (0.0605 nm) ions [26].

FESEM and EDS analyses

Figure 3 shows the micro-structure of the nanopowders obtained through field emission scanning electron microscope (FESEM) at high



magnifications for pure BST (calcined at 750°C and 850°C) and co-doped with Fe (BSTF) and Ni (BSTN) (calcined for 4 hours at 850°C) powder samples in Figures 3a-3d respectively. As was observed in previous studies, increasing the calcination temperature from 750 to 850°C leads to an increase in particle size and increasing of crystallite of BST sample which, the images in Figures 3a and 3b show an increase in grain growth with increasing calcination temperature [24]. Also, Figure 3b shows the particles are nearly cubic in nature and more crystalline. Furthermore, Images in Figures 3c and 3d clearly show that the additive of iron and nickel ions leads to a grain refining and reduce of nanoparticle size and less agglomerated, and they show well-distributed crystallites and dense nanoparticles surfaces at 850°C which, this effect is more obvious for nickel ions. The result is consistent with the results of XRD and FT-IR analyses of the prepared samples.

In order to investigate the composition of the samples, EDS analysis was used. Figure 4 shows the EDS spectra of BST, BSTF and BSTN powders calcined at 850°C. As can be seen, the characteristic X-ray radiation of each element has different energy values with various atomic compositions. In Figure 4a, the presence of Ba, Sr and Ti was detected in the spectra of pure BST, it is clearly seen that the prepared Ba_{0.06}Sr_{0.4}TiO₃ ceramic compound is only composed of Ba, Sr, Ti, and O and the pure BST is a dominant phase. Also, Figures 4b and 4c show clearly the presence of Fe and Ni in the BSTF and BSTN compositions, respectively. Table 5 shows Weight % and Atomic % of all elements present in the samples. As can be seen, the addition of iron and nickel in BST structure lead to modifying the stoichiometric ratio of elements of BST compound.

UV-Vis analysis

It is well-known that the grain size of nanoparticles and the amount and type of doping mater are important factors in determining of the electrical and optical properties of the BST [27,28]. In order to obtain

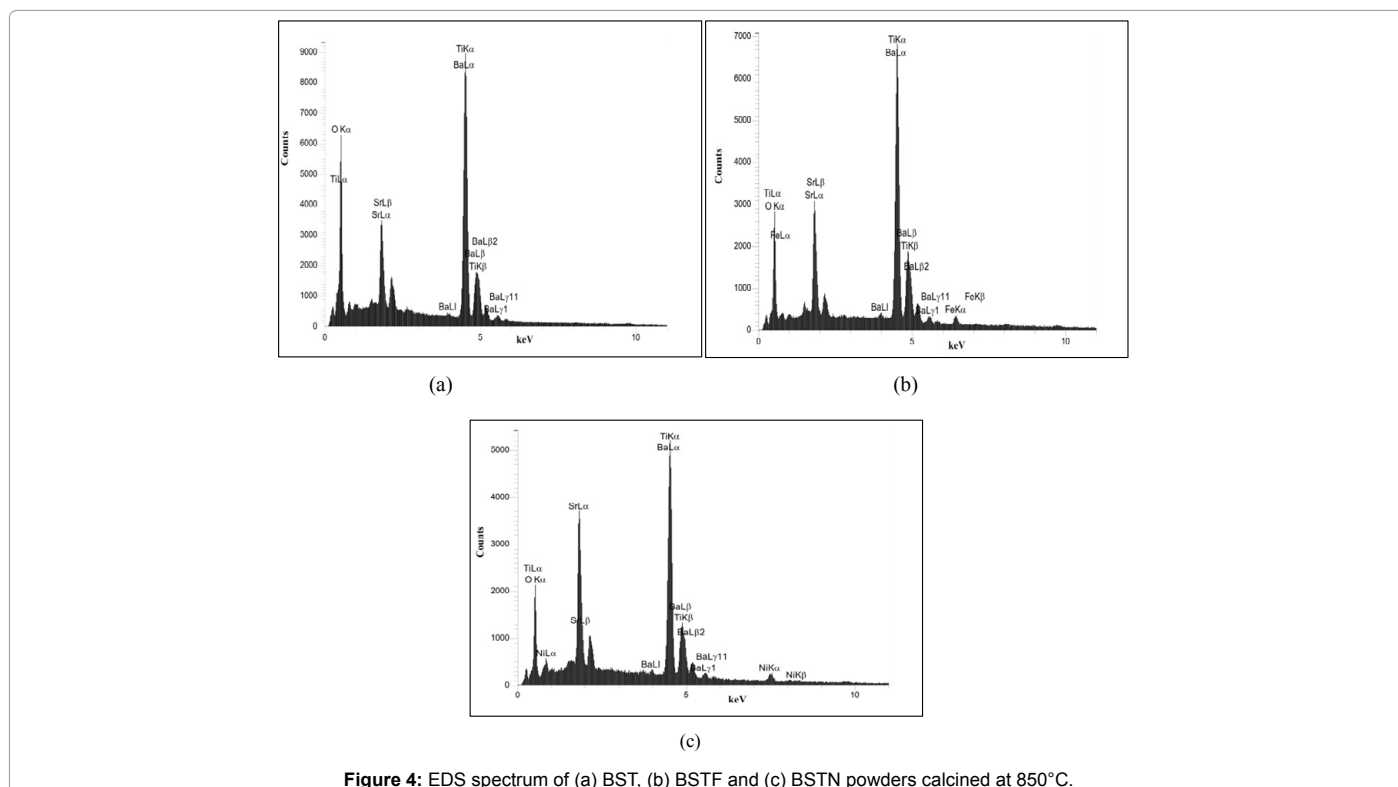


Figure 4: EDS spectrum of (a) BST, (b) BSTF and (c) BSTN powders calcined at 850°C.

Crystal system	Cubic	Angles (α, β, γ)	90.00°, 90.00°, 90.00°
Space group number	221	Calculated density	5.68
Space group	Pm-3m	Volume of cell	62.33
Lattice parameters	3.965Å, 3.965Å, 3.965Å		

Table 4: The crystallographic parameters used for the XRD pattern fitting for BST60/40 ceramics.

Element	Line	BST		BSTF		BSTN	
		Weight%	Atomic%	Weight%	Atomic%	Weight%	Atomic%
O	Kα	47.56	78.43	34.00	68.97	31.46	66.38
Ti	Kα	29.57	16.29	31.85	21.58	29.63	20.88
Fe	Kα	----	----	1.30	0.75	----	----
Ni	Kα	----	----	----	----	3.74	2.15
Sr	Lα	8.13	2.45	6.88	2.55	14.00	5.39
Ba	Lα	14.75	2.83	25.97	6.14	21.16	5.20
Total		100.00	100.00	100.00	100.00	100.00	100.00

Table 5: Weight % and Atomic % of all elements present in the BST, BSTF and BSTN samples.

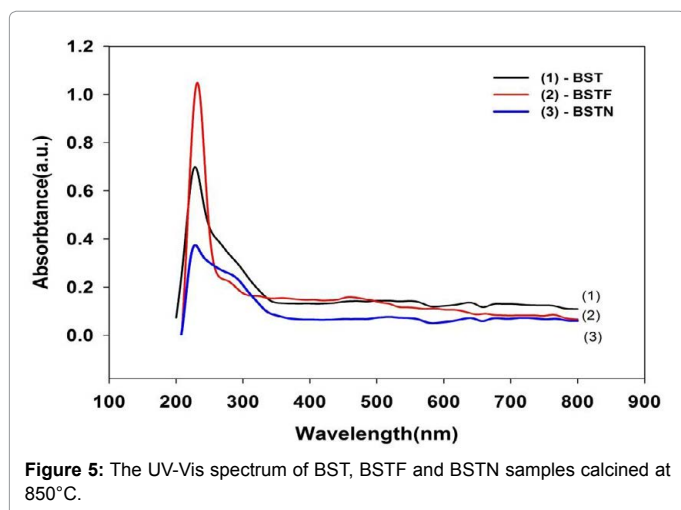


Figure 5: The UV-Vis spectrum of BST, BSTF and BSTN samples calcined at 850°C.

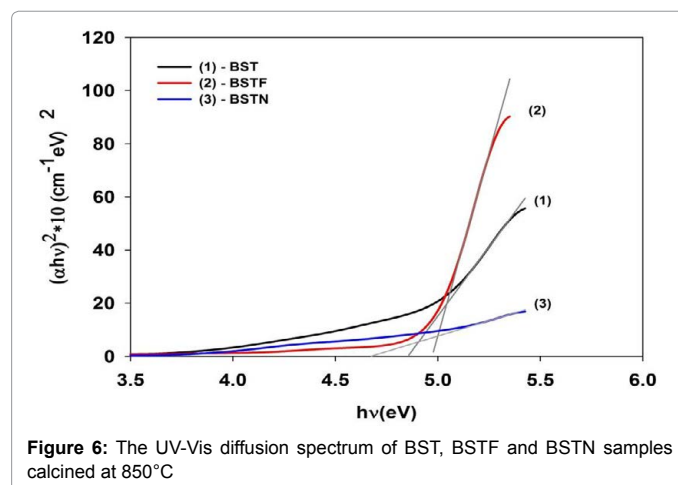


Figure 6: The UV-Vis diffusion spectrum of BST, BSTF and BSTN samples calcined at 850°C

the UV spectra of the samples initially, put some of them in methanol, and then place them for 15 minutes in an ultrasonic device to become a uniform disperse solution. Prepared solution was put in the special quartz cells and UV-Vis ray is radiated in the range of 200 to 500 nm. Figure 5 shows the absorption spectra of BST, BSTF and BSTN samples calcined at 850°C. The absorption profiles for all the samples exhibit sharp bands in the UV region. As Figure 5 clearly shows that the adding of Fe and Ni to BST structure lead to displace the edge of the absorption in the UV spectra. The wavelength corresponding to the absorbance edge for BST, BSTF and BSTN nanopowders is 228.32 nm, 231.85 nm and 228.64 nm, respectively. This means that the Fe and Ni dopant can change the optical properties of the BST nanopowders.

The band-gap energy of samples was determined by the Kubelka-Munk model and the Tauc linearization for direct allowed transitions:

$$(\alpha h\nu)^2 = c(h\nu - E_g) \quad (3)$$

where α is the absorption coefficient, $h\nu$ is the photon energy and E_g is the optical band gap. The optical band gap was determined by extrapolating the linear portion of the plot to $\alpha^2 = 0$ in the plot of the square of the absorption coefficient versus photon energy [29].

Figure 6 shows the diffusion spectrum (tauc plot) for direct transition of BST, BSTF and BSTN nanopowders calcined at 850°C. The results show that the value of the energy band gap increase with doping Fe in BST structure and decrease with doping Ni, in comparison

with pure BST nanopowder. The direct band-gap energy of BST, BSTF and BSTN nanopowders is 4.85, 4.97 and 4.67, respectively. Also, the direct band gap energy of the BST nanopowder was higher than the ones usually found in the literature of the context for BST thin film (around 3.93 eV) [30].

Conclusions

In this paper, the Ba_{0.6}Sr_{0.4}TiO₃ (BST), Ba_{0.6}Sr_{0.4}Ti_{0.9}Fe_{0.1}O₃ (BSTF) and Ba_{0.6}Sr_{0.4}Ti_{0.9}Ni_{0.1}O₃ (BSTN) Nanocrystalline were successfully synthesized by a modified sol-gel technique and studied by XRD, FT-IR, UV-Visible, FESEM, EDX techniques. FT-IR spectra and XRD pattern showed present of pure BST structure and un-wanted amount of impure phase of BaCO₃ and SrCO₃ due to doping Fe and Ni into BST structure. XRD patterns confirmed the cubic structure phase presence of the prepared samples. The average of particle size calculated from the XRD pattern was nearly 38, 36 nm and 34 for BST, BSTF and BSTN for calcination temperatures 850°C, respectively. Also, the XRD pattern showed that the adding Fe and Ni to BST structure lead to an increase of lattice parameter. XRD and FESEM investigation showed that the average grain size of the BST ceramics decreased by adding of Fe and Ni and the microstructure became uniform. EDX analysis confirmed the presence of Ba, Sr, Ti, O, Fe and Ni in the compositions. The effects of Fe and Ni dopant on the optical properties of the BST nanopowders have been studied by UV-Visible spectroscopy. The band-gap energy of BST, BSTF and BSTN nanopowders is 4.85, 4.97 and 4.67, respectively. The result shows that the Fe and Ni dopant can change the

optical properties of the BST nanopowders. Additionally, the sol-gel technique applied in this work can be used to deposit a nano thin film of BST.

References

- Jang HM, Jun YH (1997) (Ba, Sr)TiO₃ system under DC-bias field: II. Induced and intrinsic pyroelectric coefficients and figures-of-merit. *Ferroelectrics* 193: 125-140.
- Wodecka-Dus B, Lisinska-Czekaj A, Orkisz T (2007) The sol-gel synthesis of barium strontium titanate ceramics. *Mater. Sci-Poland* 25: 791-799.
- Reynolds GJ, Kratzer M, Dubs M (2012) Electrical Properties of Thin-Film Capacitors Fabricated Using High Temperature Sputtered Modified Barium Titanate. *Materials* 5: 644-660.
- Banerjee M, Mukherjee S, Maitra S (2012) Synthesis and Characterization of Nickel Oxide Doped Barium Strontium Titanate ceramics. *Ceramica* 58: 99-104.
- Sun X, Zhu B, Liu T, Li M (2006) Dielectric and tunable properties of K-doped Ba_{0.6}Sr_{0.4}TiO₃ thin films fabricated by sol-gel method. *J. Appl. Phys* 99: 084103.
- Kim KT, Kim CI (2005) The effect of Cr doping on the microstructural and dielectric properties of Ba_{0.6}Sr_{0.4}TiO₃ thin films. *Thin Solid Films* 472: 26-30.
- Battisha IK, Sayed Ahmed Farag I (2014) Structural, Magnetic and Dielectric Properties of Fe-Co Co-Doped Ba_{0.9}Sr_{0.1}TiO₃ Prepared by Sol Gel Technique. *NJGC* 4: 19-28.
- Saeed A, Ruthramurthy B, Ban TK, Hoong OB (2015) Structural and magnetic properties of iron doped barium strontium titanate ceramic synthesised using slow injection sol-gel technique. *Mater. Technol.* 30: 140-143.
- Gomez-Yan A ez C, Benitez C, Balmori-Ramirez H (2000) Mechanical activation of the synthesis reaction of BaTiO₃ from a mixture of BaCO₃ and TiO₂ powders. *Ceram. Int* 26: 271-277.
- Ahmed MA, Kamal M, Desouky El FG (2013) Synthesis and characterization of Cobalt-doped nano-structure barium strontium titanate prepared by Sol-gel process. *JASR* 9: 2432-2438.
- Somani V, Jyoti Kalita S (2007) Synthesis and Characterization of nanocrystalline Barium Strontium Titanate powder via sol-gel processing. *J. Electroceram* 18: 57-65.
- Simoesa AZ, Mouraa F, Onofrea TB (2010) Microwave-hydrothermal synthesis of barium strontium titanate nanoparticles. *J. Alloy. Compd* 508: 620-624.
- Thakur OP, Prakash C, Agrawal DK (2002) Microwave synthesis and sintering of Ba_{0.95}Sr_{0.05}TiO₃. *Mater. Lett.* 56: 970-973.
- Golego N, Studenikin SA, Cocivera M (1998) Properties of Dielectric BaTiO₃ Thin Films Prepared by Spray Pyrolysis. *Chem. Mater.* 10: 2000-2005.
- Zhong Z, Gallagher PK (1995) Combustion synthesis and characterization of BaTiO₃. *J. Mater. Res.* 10: 945-952.
- Schrey F (1965) Effect of pH on the Chemical Preparation of Barium-Strontium Titanate. *JACS* 48: 401-405.
- Harizanov O, Harizanova A (2004) Formation and characterization of sol-gel barium titanate. *Mater. Sci. Eng.* 106: 191-195.
- Brinker CJ, Hurd AJ (1992) Review of sol-gel thin film formation. *J. Non-Cryst. Solids.* 147: 424-436.
- Tangwiwat S, Milne SJ (2005) Barium titanate sols prepared by a diol-based sol-gel route. *J. Non-Cryst Solid.* 351: 976-980.
- Miller FA, Wilkins CH (1952) Infrared Spectra and Characteristic Frequencies of Inorganic Ions. *Anal. Chem.* 24: 1253-1294.
- Kao CF, Yang WD (1999) Preparation of Barium Strontium Titanate Powder from Citrate Precursor. *Appl. Organometal. Chem* 13: 383-397.
- Adekunle AS, Oyekunle JAO, Oluwafemi OS (2014) Comparative Catalytic Properties of Ni(OH) and NiO Nanoparticles Towards the Degradation of Nitrite (NO₂) and Nitric Oxide (NO). *Int. J. Electrochem. Sci.* 9: 3008-3021.
- Aal Abdel A, Hammad TR, Zawarah M (2014) FT-IR study nanostructure perovskite BaTiO₃ doped with both Fe⁺³ and Ni⁺² ions prepared by sol-gel technique. *Acta. Phys. Pol. A.* 126: 1318-1321.
- Araghi Azim ME, Shaban N, Bahar M (2016) Synthesis and characterization of nanocrystalline Barium Strontium Titanate powder by a modified sol-gel processing. *Mater. Sci-Poland* 34: 63-68.
- Golmohammad M, Nemati ZA, Sani MF (2010) Synthesis and characterization of nanocrystalline barium strontium titanate. *Materials Science-Poland.*
- Qian L, Deng H, Zhu L, Yang P (2011) Influence of Ni-dopant on structural and optical properties of Ba_{0.6}Sr_{0.4}TiO₃ thin film by sol-gel technique. *J. Chu, JPCS* 276: 012183.
- Willander M, Nur O, Israr MQ, Abou Hamad AB (2012) Determination of A.C. Conductivity of NanoComposite Perovskite Ba(1-x-y)Sr(x)TiFe(y)O₃ Prepared by the Sol-Gel Technique. *JCPT* 2: 1-11.
- Khare A, Chauhan N (2015) The effect of Mg doping on structural and luminescent properties of Barium Strontium Titanate (BST). *Physics Procedia* 76: 86-91.
- Kocanda M, Mohiudin SF, Abdel-Motaleb I (2012) An Investigation of PLD-Deposited Barium Strontium Titanate (Ba_{1-x}Sr_xTiO₃) Thin Film Optical Properties. *CSTA* 1: 17-20.
- Bobby Singh S, Sharma HB, Sarma HNK (2008) Structural properties of nano-sized barium strontium titanate (Ba_{0.6}Sr_{0.4}TiO₃) thin film. *Mod. Phys. Lett B.* 22: 693-700.